Catalysis Science & Technology

ROYAL SOCIETY OF CHEMISTRY

REVIEW

View Article Online
View Journal | View Issue

Cite this: *Catal. Sci. Technol.*, 2025, **15**, 2440

A review of reversible hydrogenation and dehydrogenation catalysts for liquid organic hydrogen carriers

Meiying Dai,[ab] Yibo Qin,[ab] Longfei Chen[ab] and Xinqing Chen *[ab]

Hydrogen energy is widely regarded as a green, low-carbon, and efficient secondary energy source with immense potential for future energy systems. As a clean alternative to the traditional fuels, its use could significantly reduce carbon emissions and contribute to a more sustainable energy landscape. However, one of the key challenges in realizing this potential is the safe and efficient storage of hydrogen. Among the various storage technologies, liquid organic hydrogen carriers (LOHCs) have emerged as a promising solution for both on-board and off-board hydrogen storage systems. LOHCs offer notable advantages, including low cost, high hydrogen storage capacity, and storage efficiency. Despite these benefits, LOHC technology faces several obstacles, such as high reaction temperatures, reliance on expensive noble metal catalysts, and the relatively low efficiency of non-precious metal catalysts during hydrogenation and dehydrogenation processes. Consequently, there has been growing interest in developing more efficient and cost-effective catalysts to overcome these limitations. This paper reviews the recent advancements in the catalytic hydrogenation and dehydrogenation of LOHCs, particularly focusing on the role of metal catalysts in enhancing the reversible hydrogenation and release of hydrogen. The insights provided are intended to guide the rational design of next-generation catalysts, which could significantly enhance the performance of hydrogen storage systems and advance hydrogen technology toward broader practical applications.

Received 10th December 2024,
Accepted 3rd March 2025

DOI: 10.1039/d4cy01483a

rsc.li/catalysis

1. Introduction

In light of rising energy demand and environmental challenges, discovering new green energy sources is essential for advancing social progress and fostering scientific and technological development. Hydrogen energy is regarded as one of the most promising clean energy sources of the 21st century, offering advantages such as high energy density, broad applicability, abundant reserves, and non-toxicity.[1,2] The concept of a "hydrogen economy," proposed in the 1970s, envisions an economic system centered around hydrogen as the primary energy carrier.[3] This system encompasses an industrial chain that includes upstream hydrogen production, midstream storage and transportation, and downstream utilization. Hydrogen, a gas at normal temperature and pressure, is characterized by its flammability, explosiveness, and tendency to diffuse easily, along with a very low volumetric density. In terms of mass energy density, 1 kg of hydrogen can replace approximately 3 kg of gasoline. However, when considering volumetric energy density, it takes about 13 000 liters of hydrogen to replace 3.79 liters of gasoline under standard conditions. This highlights an urgent need to develop innovative and effective solutions to the pressing challenges of hydrogen storage and transport.[4,5]

In 1975, Sultan *et al.*[6] proposed using a pair of liquid organic compounds with unsaturated double bonds to facilitate highly reversible hydrogenation and dehydrogenation reactions for hydrogen storage and release. This organic liquid hydrogen storage system, known as liquid organic hydrogen carriers (LOHCs), consists primarily of hydrogen-poor organic compounds ($LOHC^-$) and hydrogen-rich organic compounds ($LOHC^+$). In the catalytic hydrogenation reaction, hydrogen is stored by converting $LOHC^-$ into $LOHC^+$. Conversely, during the catalytic dehydrogenation reaction, hydrogen is released by converting $LOHC^+$ back into $LOHC^-$.[7] Notably, $LOHC^+$ compounds can store hydrogen for extended periods without self-release, making them particularly advantageous for seasonal energy storage and transportation in remote areas. As research advances, LOHCs have become increasingly significant in the field of hydrogen storage and are considered one of the most promising materials for large-scale applications in the future.[8] The hydrogen storage process utilizing LOHCs is illustrated in

[a] *CAS Key Laboratory of Low-carbon Conversion Science and Engineering, State Key laboratory of low carbon catalysis and carbondioxide utilization, Shanghai Advanced Research Institute, Chinese Academy of Sciences, Shanghai 201210, China. E-mail: chenxq@sari.ac.cn*
[b] *University of Chinese Academy of Sciences, Beijing 100049, China*

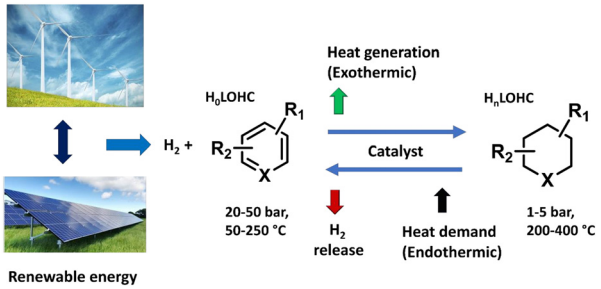

Fig. 1 The schematic of LOHCs during hydrogen storage.[9]

Fig. 1. Hydrogen is produced using surplus electricity from renewable sources such as wind, solar, and tidal energy. This hydrogen is then hydrogenated with LOHCs until the double bond is saturated, converting it into $LOHC^+$ for effective hydrogen storage. Under the influence of a catalyst, $LOHC^+$ absorbs heat, triggering a dehydrogenation reaction that releases hydrogen. The reaction typically occurs at normal pressure and at temperatures ranging from 30 °C to 420 °C, depending on the specific LOHCs and catalyst performance. The heat required for dehydrogenation can be obtained by burning the partially released hydrogen gas or from waste heat generated using equipment such as hydrogen fuel cells. After dehydrogenation, $LOHC^+$ is prepared to enter the next cycle of hydrogen storage.

The hydrogen storage capacity of LOHCs is closely linked to their hydrogen storage medium, primarily composed of carbon cyclic aromatic hydrocarbons. Key combinations include benzene/cyclohexane, toluene/methylcyclohexane, naphthalene/decahydronaphthalene, and benzyltoluene/dibenzyltoluene (DBT). Additionally, cyclic aromatic hydrocarbons containing heteroatoms, such as carbazole, indole, and quinoline, along with their derivatives, significantly contribute to hydrogen storage.[10–15] These media exhibit a high hydrogen-to-carbon ratio, high energy density, and ease of transportation, making them ideal candidates for fuel cells and laying a solid foundation for a 'hydrogen energy economy'. Furthermore, LOHCs are non-toxic, non-corrosive, and physically similar to liquefied petroleum gas, ensuring high compatibility with existing petroleum-based infrastructure and effectively reducing transportation equipment costs. To date, the hydrogenation and dehydrogenation reactions of various LOHCs have been extensively studied.[16] This paper reviews recent research on the hydrogenation, dehydrogenation, and reversible dehydrogenation of LOHCs catalyzed by metal catalysts. The aim is to provide insights that can guide the design of more effective and efficient catalysts. This work holds significant practical implications for advancing hydrogen technology, contributing to the development of more reliable and sustainable energy solutions.

2. Catalysts for hydrogenation of LOHCs

The hydrogenation reaction of LOHCs involves a balance between heat release and reduction in reaction volume. Thermodynamically, increasing the reaction pressure and decreasing the temperature enhance both conversion rates and selectivity in aromatic hydrogenation. While hydrogenation is thermodynamically favorable and exothermic, catalyst optimization primarily targets accelerated kinetics and reduced energy input, rather than overcoming fundamental thermodynamic limitations. As a result, hydrogenation processes are generally more amenable to industrialization than dehydrogenation, supported by more mature technologies. Additionally, the choice of catalyst plays a critical role in determining conversion and selectivity, making it essential for efficiency improvements. The effectiveness of hydrogenation catalysts largely relies on the active components supported by the carrier, with common catalysts divided into precious and non-precious metal types. Table 1 summarizes some of the catalysts used in the *N*-ethylcarbazole (NEC) hydrogenation reaction.

Precious metals are valued due to their excellent corrosion and oxidation resistance, high-temperature stability, and strong catalytic activity. In particular, Pt-based catalysts are regarded as highly promising for the hydrogenation of LOHCs. Tian *et al.*[32] proposed a novel method for encapsulating subnanometric Pt clusters within high thermal stability beta zeolite. The results indicate that the Pt clusters in the Pt@H-beta catalyst are influenced by the strong electronic interactions with the zeolite, which promote the transfer of active hydrogen. Pawelec *et al.*[33] loaded precious metals Pt, Pd, and Pt–Pd onto silica–alumina and β-zeolite (βZ) to catalyze the hydrogenation of toluene and naphthalene. Their results indicated that the Pt–PdH/βZ catalyst demonstrated exceptional hydrogenation activity and stability. This remarkable performance was attributed to the synergistic interaction between Pt and Pd. Ru-based catalysts are some of the most commonly employed precious metal catalysts in organic liquid hydrogenation reactions. Eblagon *et al.*[34] noted that among Ru, Pt, Pd, Rh, and non-precious metals like Ni, Ru exhibits the highest catalytic activity for NEC hydrogenation, rendering it the most effective catalyst for this reaction. Typically, Ru catalysts supported by Al_2O_3 are the most prevalent for NEC hydrogenation.[17] Ge *et al.*[5] further developed a Ru monatomic catalyst (Ru(Na)/Beta) supported on *BEA molecular sieves, demonstrating excellent activity in the NEC hydrogenation reaction. This catalyst achieved a hydrogen uptake of 5.69 wt% and a conversion rate of 99% at 100 °C and 6 MPa H_2. Their analysis of the hydrogenation process and mechanism revealed that the accelerated reaction rate was primarily due to the high dispersion of Ru atoms, the strong acidity of the molecular sieves, and the synergistic interaction between the Ru atoms and the *BEA molecular sieves (Fig. 2). Rh-based catalysts have remarkable activity in toluene hydrogenation. For example, Ali *et al.*[35] found that Rh catalysts supported on Al_2O_3 exhibited the highest catalytic activity for toluene hydrogenation at 170 °C, outperforming Pt and Ir catalysts. Additionally, Rh-based catalysts demonstrated strong performance in the hydrogenation of quinoline. Mateen *et al.*[36] synthesized a series of rhodium–copper bimetallic catalysts with varying compositions and a uniform morphology for the selective hydrogenation of quinoline, finding that the Rh_3Cu_1

Table 1 Summary of catalytic performances of different catalysts for the hydrogenation of 12H-NEC

Catalyst	Temperature (°C)	H_2 pressure (bar)	Solvent	Conversion (%)	Ref.
5 wt% Ru/Al_2O_3	170	80		100	17
5 wt% Ru/Al_2O_3 (COM)	130	70		92	18
5 wt% Ru/TiO_2	130	70		96	18
5 wt% Ru/SiO_2–Al_2O_3	130	70		96	18
5 wt% Ru on zeolite	130	70		78	18
5 wt% Ru on graphite	130	70		64	18
5 wt% Ru/AC	130	70		53	18
0.5 wt% Ru(Na)/beta	100	60		99	5
Ru–B	60	70		99	19
5 wt% Ru/Al_2O_3–YH_3	150	13		55	20
1 wt% Pd/Al_2O_3	180	70		100	21
1 wt% $Pd/LaNi_5$	180	70		100	21
Pd black (COM)	130	70	Cyclohexane	47	22
Pd_2Ru@SiCN	110	20		98	23
5 wt% Pt/AC	130	70		0.6	18
Pt black (COM)	130	70	Cyclohexane	89	22
0.1 wt% Rh/γ-Al_2O_3	160	60		99	24
65 wt% Ni/SiO_2–Al_2O_3 (COM)	130	70		93	18
65 wt% Ni/AC	130	70		33	18
RANEY®-Ni	180	50		79	25
Ru–Ni_1Al_2-LDO_{300}	150	80		100	26
5 wt% Ni/Al_2O_3–YH_3	150	30		100	20
Ni_4Mo/AC	150	80		100	27
Ni/MCM-41(500)	180	50		100	28
Ru–Ni/TiO_2	150	70		100	29
Co–B/Al_2O_3–YH_{3-x}	180	100		>94	30
Co@Ru/NGC	130	60		100	31

catalyst achieved the best activity and selectivity, even surpassing those of a comparable Rh/C catalyst. This enhanced performance is attributed to the synergistic effect between rhodium and copper, highlighting the potential of bimetallic nanocrystals as effective catalysts for selective hydrogenation of quinoline and similar substrates.

Although precious metal catalysts are highly efficient, they are expensive compared to non-precious metal catalysts. As a result, the use of non-noble metal supported catalysts, such as Ni and Co, in LOHCs has attracted considerable attention from researchers. Liu *et al.*[24] developed a Rh–Ni bimetallic catalyst with an ultra-low Rh content of 0.1 wt% on cost-effective γ-Al_2O_3. This catalyst achieved a hydrogen storage rate of 5.63% within 2 hours, which is close to the theoretical hydrogen storage capacity of 5.8 wt% (Fig. 3). Despite the low Rh content, the catalyst benefits from a synergistic effect between Rh and Ni, enhancing the reducibility of NiO supported on the catalyst and facilitating the formation of smaller Ni nanoparticles. Furthermore, the electron transfer between the bimetallic Rh–

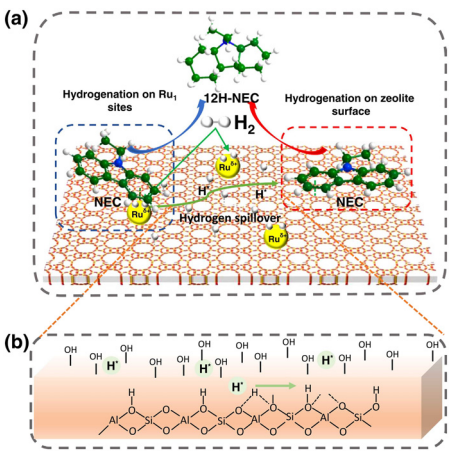

Fig. 2 (a) The hydrogenation pathways of NEC; (b) mechanism of transfer of H species on Ru(Na)/beta.[5]

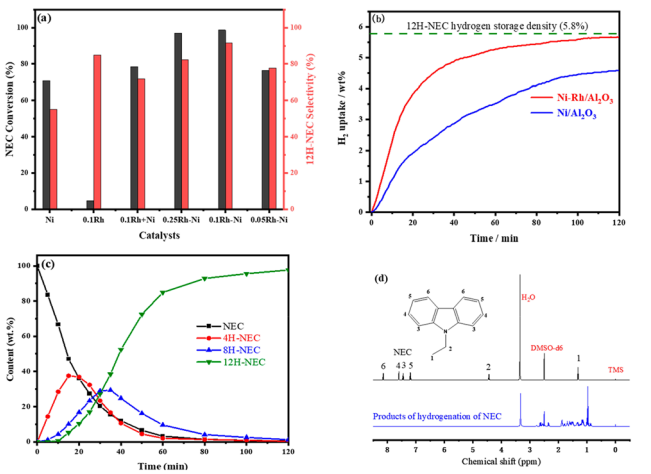

Fig. 3 (a) Catalytic performances of catalysts (160 °C, 60 bar, 5 g NEC, 0.25 g catalyst, 1 h); (b) hydrogenation kinetic curves of NEC on different catalysts (160 °C, 6 MPa, 5.0 g NEC, 250 mg Ni/γ-Al_2O_3 or 0.1Rh-Ni/γ-Al_2O_3); (c) time-dependent product distribution for NEC hydrogenation of the 0.1Rh–Ni/γ-Al_2O_3 catalyst (160 °C, 6 MPa); (d) 1H NMR spectrum of the products of hydrogenation of NEC over the 0.1Rh-Ni/γ-Al_2O_3 catalyst.[24]

Ni nanoparticle structures on the catalyst support also plays a significant role in its outstanding catalytic performance. Lu *et al.*[37] prepared PtCo and PtNi bimetallic catalysts as well as Co, Ni and Pt monometallic catalysts on γ-Al_2O_3 by an impregnation method to evaluate the hydrogenation of benzene and cyclohexene at low temperatures and atmospheric pressure. The results showed that the PtCo catalysts were significantly more active for the hydrogenation of benzene, while the PtNi catalysts were more active for the hydrogenation of cyclohexene. The addition of small amounts of Pt can improve the chemisorption capacity and make the reduction of Co or Ni easier, especially for Co-based catalysts. Additionally, Liu *et al.*[38] prepared an SBA-15 supported Ru–Co alloy nanoparticle catalyst, which demonstrated efficient hydrogen storage on organic liquid carriers such as NEC, DBT, and acenaphthylene. The hydrogenation capability of La–Ni/Al_2O_3 nanoparticle catalysts, prepared by Zhu *et al.*,[39] surpasses that of most advanced commercial catalysts. This enhanced performance is attributed to the uniform formation of ultrafine nanoparticles induced by La species, the prevention of undesirable compositional changes, the optimization of microstructure distribution, and the balanced dispersion of acid sites.

In conclusion, the activity and selectivity of catalysts in LOHCs can be improved by optimizing support materials and enhancing catalyst dispersion. Furthermore, exploring synergistic interactions between catalysts may lead to more efficient hydrogenation performance. The development of bimetallic catalysts, incorporating a noble metal to boost the hydrogenation activity of non-noble metals, not only enhances overall catalyst stability but also reduces costs, offering promising potential for future advancements in hydrogenation technology.

3. Catalysts for dehydrogenation of LOHCs

While the hydrogenation of certain organic liquids can be accomplished under mild conditions, achieving reversible dehydrogenation under the same conditions remains challenging. Under specific pressure conditions, the rate of dehydrogenation is primarily accelerated by increasing the reaction temperature. The catalytic performance of dehydrogenation catalysts is influenced by factors such as the catalyst support, the active metal components, and the structural sensitivity of the catalysts. Dehydrogenation catalysts are typically classified into two categories: precious metal catalysts and non-precious metal catalysts. Table 2 summarizes some of the catalysts used in the NEC dehydrogenation reaction.

Precious metals like Pt and Pd are particularly valued due to their exceptional catalytic dehydrogenation properties, including high activity, selectivity, and resistance to deactivation. These metals are typically supported on materials such as Al_2O_3, SiO_2 and $Mg(OH)_2$ to enhance their stability and performance. Pd-based catalysts have demonstrated superior catalytic performance in the dehydrogenation reaction of 12H-NEC compared to other noble metal catalysts.[43] Ge *et al.*[41]

Table 2 Summary of catalytic performances of different catalysts for the dehydrogenation of 12H-NEC

Catalyst	Temperature (°C)	Solvent	Conversion (%)	Ref.
Pd@SiCN	180		93	40
Pd/MgO	180		71	41
Pd/rGO	180		100	42
0.5 wt% Pd/$Mg(OH)_2$	180		100	41
Pd/N–C_{HNO_3}	180		100	43
5 wt% Pd/C	170		100	44
5 wt% Pd/TiO_2	180		58	45
5 wt% Pd/Al_2O_3(COM)	180		100	46
2.5 wt% Pd/rGO–EG	180	Decalin	100	47
5 wt% Rh/Al_2O_3(COM)	180		11	46
5 wt% Rh/TiO_2	180		30	45
0.2 wt% Rh–1 wt% Pd/γ-Al_2O_3	180		96	47
$Rh_1Pd_{1.3}$/rGO	180		57	48
$Ru_1Pd_{1.3}$/rGO	180		84	48
5 wt% Ru/Al_2O_3(COM)	180		71	46
5 wt% Ru/TiO_2	180		2	45
5 wt% Pt/Al_2O_3(COM)	180		100	46
5 wt% Pt/TiO_2	180		64	45
$Pd_{1.2}Cu$/rGO	180		100	49
$Au_1Pd_{1.3}$/rGO	180		100	50
$Pd1Co_9$/beta	180		100	51
1 wt% Pd_1Co_5/Al_2O_3	180		99.3	52
1 wt% Co/Al_2O_3	180		6.99	53
Pd_3Ni_1/SiO_2	180		100	53

capitalized on the strong alkalinity of magnesium hydroxide nanosheets to develop two-dimensional magnesium hydroxide nanosheets (Pd/$Mg(OH)_2$) loaded with Pd clusters. This innovative approach enabled the formation of stable Pd clusters (Pd^{n+}–OH), effectively lowering the dehydrogenation barrier and significantly enhancing the dehydrogenation performance (Fig. 4). With a metal loading of just 0.5 wt%, this catalyst achieved a remarkable 100% conversion of 12H-NEC and a hydrogen release of 5.72 wt%. In their study of 12H-NEC dehydrogenation, Wang *et al.*[42] found that the conversion rate and selectivity were strongly influenced by the facet structure of Pd metal, with the {100} facet exhibiting exceptional activity. Moreover, in their study on the dehydrogenation of N-heterocyclic LOHCs, Li *et al.*[54] highlighted that the interaction between Pd^0 and $Pd^{\delta+}$ electrons is crucial for enhancing both the efficiency and stability of the dehydrogenation process. Additionally, the preparation methods employed can result in varying catalytic properties. Zhu *et al.*[55] explored this by

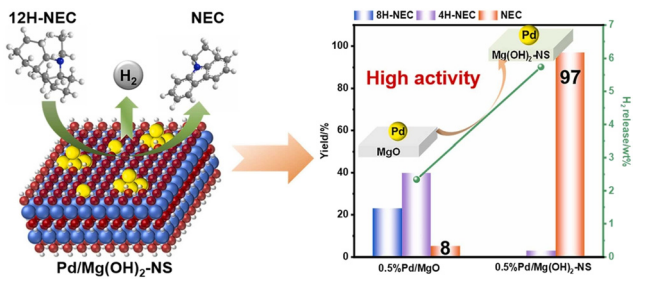

Fig. 4 The dehydrogenation pathways of NEC on Pd/$Mg(OH)_2$.[40]

synthesizing a series of Pd–Ru loaded catalysts using both double reduction and $NaBH_4$ reduction methods. Their findings revealed that the catalysts prepared *via* the double reduction method showcased enhanced catalytic performance and recyclability. Pt exhibits a higher hydrogen recombination ability compared to Ru, Rh, and Pd,[56] and it also demonstrates exceptional activity in dehydrogenation reactions. Li *et al.*[57] believed that Pt-based catalysts are the most effective for the selective dehydrogenation of methylcyclohexane to toluene, as they can efficiently activate C–H bonds while reducing C–C bond cleavage. Ahn *et al.*[58] developed a Pt catalyst supported on ordered mesoporous silica for the dehydrogenation of methylcyclohexane (Pt/KIT-6). This catalyst features a higher specific surface area, increased pore volume, improved Pt dispersion, and a narrower particle size distribution. As a result, Pt/KIT-6 demonstrates a higher LOHC conversion rate and a faster hydrogen production rate compared to conventional Pt/SiO_2 and Pt/Al_2O_3 catalysts, along with greater hydrogen selectivity and stability. This highlights the importance of controlling catalyst surface properties in LOHC dehydrogenation. Han *et al.*[59] demonstrated that the distribution of Pt (*i.e.*, egg-shell *vs.* uniform structure) resulting from the synthesis method affects the particle size and dispersion of Pt, which in turn influences the electron density of the metal. However, precious catalysts are expensive, less stable, and prone to deactivation. Therefore, developing improved catalysts that are both durable and cost-effective is essential for advancing organic liquid dehydrogenation.

Non-precious metals such as Cu and Ni are utilized for dehydrogenation. The small differences in lattice parameters and atomic radii between Cu and Pd facilitate the formation of a diverse range of alloying structures, allowing for precise tuning of both activity and selectivity in catalytic reactions. Wang *et al.*[49] developed a series of bimetallic Pd–Cu catalysts with varying ratios, utilizing reduced graphene oxide as a support for the dehydrogenation reaction of 12H-NEC. Among these catalysts, the $Pd_{1.2}$Cu/rGO variant exhibited both the lowest precious metal content and the highest dehydrogenation activity. Further investigation into the underlying mechanisms revealed that two critical factors influencing catalytic performance were the average particle size and the electron transfer between Pd and Cu. Building on this, Tan *et al.*[60] explored a novel Cr-doped, Mn-promoted Cu-based catalyst for methanolysis. Their results demonstrated that this catalyst achieved an impressive 84.3% hydrogen selectivity at complete methanol conversion when the Cr molar ratio was set at 0.4, alongside remarkable long-term stability over 80 hours of reaction. This performance surpassed that of most previously reported transition metal-based catalysts. Mechanistic studies indicated that Mn doping enhanced the reduction and dispersion of Cu species while modulating the electronic properties of surface Cu sites. Moreover, a moderate level of Cr doping promoted the formation of smaller Cu particles and reduced the acidity of the catalyst surface, facilitating the development of abundant interfacial Cu^+ sites. In addition, researchers enhanced the catalytic performance of nickel-based catalysts by doping them with precious metals. For instance, Li *et al.*[61] immobilized ultrafine, highly dispersed Pd nanoparticles onto Ni and N co-doped carbon materials using wet chemical reduction. The resulting Pd/Ni@NC-10 catalyst demonstrated exceptional catalytic performance for the dehydrogenation of *N*-phenylcarbazole, with 100% conversion, 81.9% selectivity, and 6.48 wt% hydrogen release. They found that the doped Ni and N species worked synergistically to enhance the dispersion of Pd nanoparticles and modulate the electronic states around Pd, thereby accelerating the rate-limiting step in the dehydrogenation process. The strong interactions between the Pd nanoparticles and the Ni and N co-doped carbon materials were key to the increase in dehydrogenation efficiency. Furthermore, Zhang *et al.*[62] conducted a systematic study of the complete dehydrogenation mechanism on Pt(111) and Ni(111) catalyst surfaces. Their calculations revealed that the step from 3H-NEC to 2H-NEC is rate-limiting, with Ni displaying lower catalytic efficiency compared to Pd. This difference is closely tied to the higher d-band center and narrower d-band distribution of Ni. Methylcyclohexane undergoes demethylation at both metallic and acidic sites, producing cyclohexane and methane. Further dehydrogenation of cyclohexane leads to the formation of benzene, along with incomplete dehydrogenation products such as cyclohexene and cyclohexadiene.[63] These are unwanted by-products. Gao *et al.*[64] found that the application of TiO_2 carriers could significantly reduce the acidity of the catalysts, and the Ni particles could be stably dispersed on the carriers, which could effectively improve the selectivity of toluene.

These findings suggest that a deeper understanding of the dehydrogenation mechanisms in catalysts can provide valuable insights for optimizing catalytic performance, offering a foundation for future experimental studies aimed at improving the efficiency of dehydrogenation catalysts.

4. Catalysts for reversible hydrogenation of LOHCs

The organic liquid reversible hydrogenation and dehydrogenation system offers a streamlined approach by combining both the hydrogenation and dehydrogenation of organic liquid carriers using the same catalyst in a single reactor. This integrated system provides significant economic and ecological advantages, as it simplifies the process of storing and releasing hydrogen, making it especially suitable for stationary applications in renewable energy storage and continuous energy supply. Despite these benefits, most catalysts developed in recent years for LOHCs have been limited to either hydrogenation or dehydrogenation, preventing efficient operation in both phases of the process. As a result, researchers are increasingly focusing on the design of advanced catalysts capable of driving reversible hydrogenation and dehydrogenation. Fig. 5 provides a summary of the various types of catalysts utilized by NEC in reversible hydrogenation and dehydrogenation reactions.

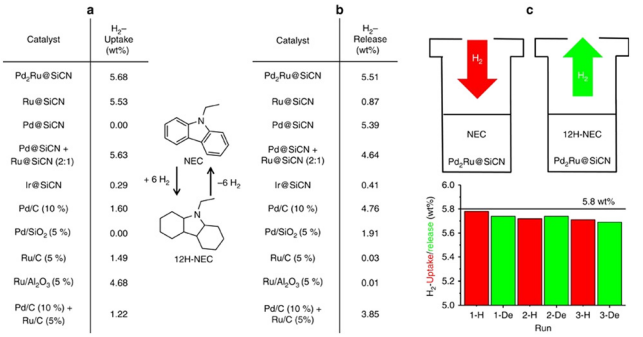

Fig. 5 Catalyst reversible hydrogen storage in NEC. (a) Hydrogenation of NEC to 12H-NEC (110 °C, 20 bar, 1 mmol NEC, 0.52 mol% active metal, 36 h); (b) dehydrogenation of 12H-NEC to NEC (180 °C, 2 mmol 12H-NEC, 0.52 mol% active metal, 7 h); (c) catalyst reusability and reversible hydrogen storage in NEC (1 g *N*-ethylcarbazole, 200 mg Pd_2Ru@SiCN, 0.52 mol% active metal, hydrogenation: 110 °C and 20 bar H_2, 36 h, dehydrogenation: 180 °C and 20 h).[62]

4.1 Noble metal catalysts

In the field of hydrogen storage, reversible dehydrogenating metal catalysts are essential for facilitating the release and uptake of hydrogen in LOHCs. These catalysts, often comprising transition metals such as Rh, Pt, Ru, and Pd, are designed to enable both the dehydrogenation of hydrogen-rich compounds and the subsequent dehydrogenation of the dehydrogenated molecules. The efficiency of these catalysts relies on their ability to alternately bind and release hydrogen atoms without substantial degradation over multiple cycles. Supported on materials like Al_2O_3 or CeO_2, they ensure not only high catalytic activity but also enhanced thermal stability and resistance to sintering. Their reversibility is critical for the practical application of LOHCs, allowing for the cyclic storage and release of hydrogen under moderate conditions while minimizing energy losses.

Pd-based catalysts are widely regarded as some of the most suitable bifunctional catalysts for N-heterocyclic hydrogenation and dehydrogenation, though their catalytic activity still requires improvement. Li *et al.*[65] enhanced Pd/Al_2O_3 by introducing the additive CeO_2, resulting in the Pd/CeAl-20 catalyst, which demonstrated outstanding performance in the reversible hydrogenation and dehydrogenation of *N*-propylcarbazole. Mechanistic analysis revealed that CeO_2 improved the dispersion of Pd nanoparticles on the support, weakened the interaction between Pd particles and the carrier, and suppressed the formation of PdO. Additionally, the Pd–O–Ce structure modulated the electronic state of Pd, highlighting the importance of the active site size and the chemical microenvironment for reversible hydrogenation and dehydrogenation in organic liquids. The preparation method of the catalyst's carrier also plays a critical role in determining its catalytic performance. Lee *et al.*[66] used solvothermal synthesis to create hierarchical titanate nanosheet (HTN) carriers for Pd catalysts. Their results showed that Pd/HTN had a hydrogen uptake three times higher than that of other Pd catalysts. Density functional theory (DFT) calculations indicated that Pd/HTN exhibited a higher density of acidic sites and oxygen vacancies compared to TiO_2 produced by other methods. Pd can also be combined with other metals to form bimetallic catalysts, which further enhance catalytic activity in reversible hydrogenation and dehydrogenation reactions. Zhu *et al.*[67] further developed a bifunctional Ru–Pd/Al_2O_3 catalyst using the impregnation–hydrogen reduction method. This catalyst exhibited superior dehydrogenation activity compared to Pd/Al_2O_3, demonstrating that the positive synergistic effect between Pd and Ru nanoparticles enhanced its catalytic activity. Yang *et al.*[68] developed a Pd-loaded catalyst, Pd/Al_2O_3–YH_3, which exhibited enhanced stability when interacting with NEC. By leveraging the promotional effect of rare-earth hydrides, the catalyst demonstrated improved performance in the hydrogenation and dehydrogenation reactions of LOHCs, achieving a hydrogen storage capacity of over 5.5 wt%. This innovative approach highlights the potential of rare-earth hydrides to significantly boost catalytic efficiency in hydrogen storage systems.

Pt/Al_2O_3 catalysts are not only among the most commonly used for the dehydrogenation of organic liquids, but they also play a critical role in reversible hydrogenation and dehydrogenation reactions. Zhang *et al.*[69] demonstrated that Pt-based catalysts exhibited remarkable activity and stability in the methylcyclohexane–toluene–hydrogen cycle, achieving a hydrogen release rate of 445.3 mmol g_{Pt}^{-1} min^{-1} with a 92.26% conversion of methylcyclohexane, and a hydrogen storage rate of 1271 mmol g_{Pt}^{-1} min^{-1} at toluene conversions exceeding 99.9%. Chiyoda developed a Pt/Al_2O_3-based hydrogen storage system that utilizes the methylcyclohexane/toluene reversible hydrogenation cycle, showcasing unique advantages in hydrogen storage and transport.[70] Shi *et al.*[71] optimized the Pt/Al_2O_3 catalyst loading in the H0-DBT/H18-DBT system at 3 wt%, achieving successful integration of hydrogenation and dehydrogenation at optimal temperatures of 140 °C and 270 °C, respectively, with minimal side reactions. Chen *et al.*[72] also utilized Pt-based catalysts for the reversible hydrogenation and dehydrogenation of methylcyclohexane, developing a highly efficient Pt_1/CeO_2 catalyst composed of single Pt atoms with adjacent oxygen vacancies on the CeO_2 surface. This catalyst demonstrated unique catalytic properties, with reaction rates 309 times higher than those of conventional Pt nanoparticle-based systems. Mechanistic studies revealed that the exceptional performance of Pt_1/CeO_2 was due to a synergistic interaction between Pt atoms and the CeO_2 carrier, which enabled redox coupling between Pt and Ce ions. This interaction facilitated the adsorption, activation, and reaction of large molecules like cyclohexane and methylcyclohexane, driving hydrogen extraction and addition without requiring multiple active sites. In conclusion, Pt-based catalysts have proven highly effective for reversible hydrogenation and dehydrogenation of organic liquids, and their application is increasingly being adopted in practical hydrogen storage systems.

(a)

Catalysts	H_2-Uptake /wt.%
1%Rh/γ-Al_2O_3	5.75
1%Ru/γ-Al_2O_3	4.45
1%Ir/γ-Al_2O_3	2.02
1%Pd/γ-Al_2O_3	0.45
1%Rh/SiO_2	3.11
1%Rh/C	0.00
1%Rh/TiO_2	0.00
1%Rh/MCM-41	1.38
1%Rh-1%Pd/γ-Al_2O_3	5.53
0.8%Rh-1%Pd/γ-Al_2O_3	5.49
0.6%Rh-1%Pd/γ-Al_2O_3	5.46
0.4%Rh-1%Pd/γ-Al_2O_3	3.49
0.2%Rh-1%Pd/γ-Al_2O_3	1.29

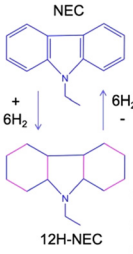

(b)

Catalysts	H_2-Release /wt.%
1%Rh/γ-Al_2O_3	2. 41
1%Ru/γ-Al_2O_3	1. 08
1%Ir/γ-Al_2O_3	1. 25
1%Pd/γ-Al_2O_3	5. 59
1%Rh/SiO_2	1. 09
1%Rh/C	1. 86
1%Rh/TiO_2	1. 46
1%Rh/MCM-41	1. 39
1%Rh-1%Pd/γ-Al_2O_3	2. 10
0.8%Rh-1%Pd/γ-Al_2O_3	3. 94
0.6%Rh-1%Pd/γ-Al_2O_3	5. 48
0.4%Rh-1%Pd/γ-Al_2O_3	5. 49
0.2%Rh-1%Pd/γ-Al_2O_3	5. 55

Fig. 6 Catalyst reversible hydrogen storage in NEC. (a) Hydrogenation of NEC to 12H-NEC (160 °C, 60 bar, 5 g NEC, 0.5 g catalysts, 1 h); (b) dehydrogenation of 12H-NEC to NEC (180 °C, 5 g 12H-NEC,0.5 g catalysts, 4 h).[72]

Bi-precious metal catalysts are of great significance in the reversible dehydrogenation reaction. Hu *et al.*[73] identified specific ruthenium pincer catalysts, along with suitable bases, which efficiently catalyze the conversion of 2-aminoethanol into cyclic dipeptides while simultaneously releasing hydrogen. This process was achieved either in the absence of solvents or with minimal solvent usage. The catalysts demonstrated excellent stability and reusability, maintaining their effectiveness across multiple dehydrogenation–hydrogenation cycles. The bimetallic Pd_2-Ru@SiCN catalyst, developed by Forberg *et al.*,[74] demonstrated exceptional performance for both hydrogen release and uptake in *N*-heterocyclic compounds. The hydrogen storage system efficiently hydrogenated NEC to 12H-NEC at 110 °C and 20 bar H_2 pressure, achieving 45.7 wt% of its storage capacity. Following this, the reaction mixture was heated to 180 °C in an oil bath, resulting in the release of 5.7 wt% of hydrogen within 20 hours. Notably, after three cycles, no significant decline in catalytic activity or hydrogen storage capacity was observed. Xue *et al.*[75] conducted extensive testing on a range of Pd–and Rh-based bimetallic catalysts to assess their performance in reversible hydrogenation and dehydrogenation reactions with NEC (Fig. 6). Notably, a reusable bimetallic Pd–Rh nanoparticle catalyst stood out due to its ability to efficiently facilitate both the hydrogenation of NEC and the dehydrogenation of 12H-NEC. This system achieved a maximum hydrogen uptake of 5.46 wt% and a maximum hydrogen release of 5.48 wt% at temperatures between 160 °C and 180 °C, allowing multiple reversible high-weight hydrogen storage and release cycles within short reaction times. Both *in situ* and non-*in situ* characterization showed that the catalyst's excellent performance was due to the synergistic interaction between Pd and Rh nanoparticle clusters on γ-Al_2O_3.

4.2 Other metal catalysts

Currently, the use of noble metals in organic liquid reversible dehydrogenation catalysis remains a significant barrier to large-scale industrial application. While non-precious metal catalysts are generally more cost-effective, their activity and stability typically fall short when compared to noble metal catalysts. As a result, developing efficient catalysts for reversible dehydrogenation without relying on expensive metals remains a key challenge. Among non-precious metals, Ni and Co are commonly utilized in reversible dehydrogenation processes, offering a promising avenue for further exploration and improvement.

Ni-based catalysts play a crucial role in the reversible catalysis of organic liquids. Yu *et al.* systematically studied the electronic structure and catalytic properties of $LaNi_5$ alloy[76] and its modified versions ($LaNi_{5-x}Al_x$ (ref. 77) and Pd/$LaNi_5$ (ref. 21)). Their findings showed that the synergistic effect between excess Ni and $LaNi_{5.5}$ is key to catalyzing reversible hydrogen storage in NEC. XPS and HR-TEM analysis confirmed that $LaNi_{5.5}$ particles possess a core–shell structure with Ni nanoparticles on the surface, which enhances hydrogen transport and catalytic activity. Additionally, the electronic interaction between Ni in the $LaNi_{5.5}$ particles and the $LaNi_5$ core regulates the electronic state of surface Ni, boosting the catalytic performance. Yu *et al.* also deposited Pd onto $LaNi_5$ by electrochemical displacement, forming a Pd/$LaNi_5$ interface. XPS and XANES analyses revealed electron transfer between Pd and Ni, resulting in electron-rich Ni and electron-deficient Pd species, which significantly improved the hydrogenation and dehydrogenation properties of NEC. This highlights the critical role of the Pd/$LaNi_5$ interface in the catalytic reaction. In their study of $LaNi_{5-x}Al_x$ nanoparticles, Al doping further enhanced the catalytic performance by modulating the electronic structure and hydrogenation potential. DFT calculations showed that Al doping leads to electron transfer from Al to Ni, reducing the adsorption energy and reaction barrier of hydrogenation intermediates, thus increasing hydrogen availability. In addition, Xue *et al.*[78] developed a Pd1Ni/γ-Al_2O_3 bimetallic catalyst, which contained a mere 0.05 wt% of Pd alongside the non-precious metal nickel. This catalyst was designed for the reversible hydrogenation and dehydrogenation of propylcarbazole. Despite the ultra-low Pd content, the catalyst exhibited dehydrogenation performance superior to that of a 1% Pd catalyst, and its hydrogenation efficiency was comparable to that of a 1% Ru catalyst (Fig. 7). This remarkable catalytic efficiency is largely credited to the introduction of Pd atoms, which increased the valence state of Ni. This shift altered the d-band center of Ni, bringing it closer to the Fermi energy level, thereby enhancing adsorption, reaction energy, and kinetics—ultimately boosting overall catalytic performance. In conclusion, Ni-based catalysts demonstrate significant potential for hydrogen storage applications, offering robust performance and stability. These advancements pave the way for the development of more efficient and cost-effective hydrogen storage systems.

Xue *et al.*[79] further advanced the development of catalysts for the reversible dehydrogenation of NEC by creating an atomic dispersion of Rh and Co nanoparticles, building on previous research involving Ni-doped non-precious metal catalysts. The resulting Rh_1Co structure maximized the utilization of Rh, enabling multiple cycles of efficient hydrogen uptake and release. Notably, the catalyst achieved complete hydrogenation (100%) at a remarkably low temperature of 90 °C, one of the

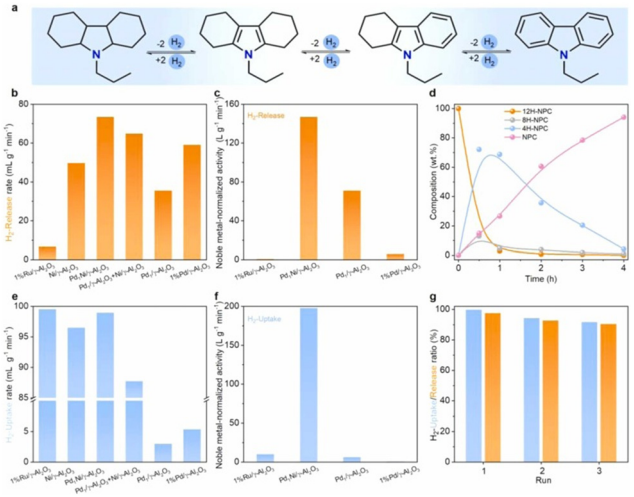

Fig. 7 Comparison of the catalytic performance of hydrogenation and dehydrogenation. (a) Hydrogenation and dehydrogenation reaction pathways of NPC; (b) dehydrogenation reaction of 12H-NPC over different catalysts (180 °C, 1 h, 5 g reactant, 0.5 g catalyst); (c) Noble metal-normalised activity for H_2-release; (d) distribution of 12H-NPC dehydrogenation products over $Pd_1Ni/\gamma\text{-}Al_2O_3$ catalysts as a function of time (180 °C, 5.0 g reactant, 0.5 g catalyst); (e) hydrogenation of NPC over $Pd_1Ni/\gamma\text{-}Al_2O_3$ catalysts on different catalysts. Reaction conditions (60 bar, 5 g reactant, 0.5 g catalyst, 1 h); (f) noble metal-normalized activity for H_2-uptake; (g) catalyst reusability test: 0.5 g catalyst, 5.0 g NEC.[75]

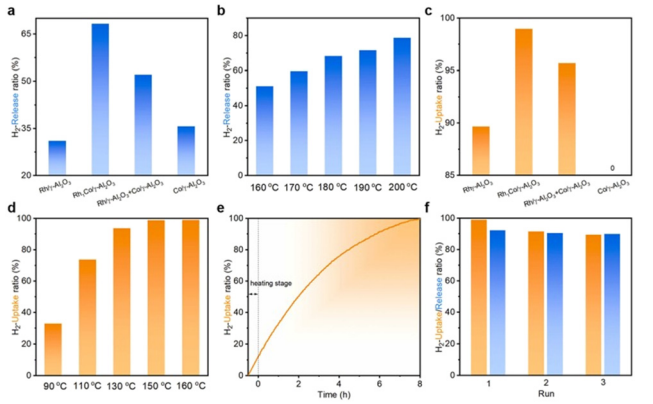

Fig. 8 Catalytic performance comparison for hydrogenation and dehydrogenation. (a) Dehydrogenation of 12 H-NEC on different catalysts (180 °C, 2 h, 5.0 g reactant, 0.5 g catalyst); (b) dehydrogenation of 12 H-NEC on $Rh_1Co/\gamma\text{-}Al_2O_3$ catalysts at different temperatures (5.0 g reactant, 0.5 g catalyst, 2 h); (c) hydrogenation of NEC on different catalysts (160 °C, 60 bar, 5 g reactant, 0.5 g catalyst, 1 h); (d) hydrogenation of NEC on $Rh_1Co/\gamma\text{-}Al_2O_3$ catalysts at different temperatures (60 bar, 5 g reactants, 0.5 g catalyst, 1 h); (e) hydrogenation of NEC on $Rh_1Co/\gamma\text{-}Al_2O_3$ catalysts (90 °C, 60 bar, 5 g reactant, 0.5 g catalyst); (f) catalyst reusability test: 0.5 g catalyst, 5.0 g NEC; hydrogenation: 60 bar, 5 g reactant, 0.5 g catalyst, 1 h; dehydrogenation: 200 °C, 5.0 g reactant, 0.5 g catalyst, 6 h.[76]

lowest temperatures reported for total hydrogenation of NEC (Fig. 8). This highlights the potential of Rh-based catalysts to enhance the synergistic effects of bimetallic or alloy catalysts, significantly improving performance in reversible dehydrogenation processes for organic liquids. In a related study, Wu *et al.*[80] introduced a Co-based catalyst driven by yttrium hydride (YH_{3-x}) for the reversible hydrogenation and dehydrogenation of NEC. This catalyst achieved a reversible hydrogen storage capacity of over 5.5 wt% at temperatures below 473 K, with favorable reaction kinetics. It is the first high-activity, non-precious metal catalyst for both NEC hydrogenation and 12H-NEC dehydrogenation. Mechanistic studies revealed that YH_{3-x} facilitates reversible hydrogen transfer during these reactions, acting as both an H donor and acceptor due to its tunable hydrogen chemical potential. This innovative approach opens new avenues for promoting multifunctional hydrogen transfer reactions using conventional metal hydrides.

In conclusion, while research on non-noble metal catalysts for reversible dehydrogenation remains limited, it presents a promising area for future exploration. Continued advancements in this field could lay a crucial foundation for the efficient storage and transport of hydrogen energy.

5. Conclusions and perspectives

The gradual depletion of non-renewable resources, coupled with the ever-increasing global demand for energy, is driving humanity to seek out new, sustainable energy alternatives. Among these, hydrogen stands out as a particularly promising option, thanks to its clean energy profile. However, the efficient storage and transportation of hydrogen present significant challenges, both in terms of cost and safety. In response, LOHCs offer a compelling solution by enabling the more efficient and secure handling of hydrogen.

This paper provides an overview of the catalysts used in LOHCs, focusing on both noble and non-precious metal catalysts for hydrogenation, dehydrogenation, and reversible addition–dehydrogenation reactions. Additionally, it assesses the strengths and weaknesses of different catalytic systems, particularly in terms of storage capacity, stability, and catalytic performance. These focused catalysts serve as a foundation for future research, providing valuable models for the development of next-generation LOHC candidate catalysts. The economic feasibility and scalability of LOHC catalysts are crucial for practical application. While precious metal catalysts (*e.g.*, Ru, Pt) offer high activity and stability, their high cost (*e.g.*, Ru: \$30 per g) and metal load (typically 5 wt%) limit large-scale use. Non-precious metal catalysts (*e.g.*, Ni: \$0.02 per g, Co: \$0.05 per g) are much cheaper but often lack sufficient activity and stability, requiring complex modifications (*e.g.*, bimetallic coordination, support optimization). Recent advances, such as Pd–Ni bimetallic catalysts, have shown promise in reducing precious metal use without sacrificing performance. For example, the $Pd–Ni/\gamma\text{-}Al_2O_3$ catalyst with just 0.05 wt% Pd achieves dehydrogenation efficiency comparable to a 1 wt% Ru catalyst, cutting costs by over 90%. However, scaling up atomically dispersed precious metal catalysts like Ru monoatoms remains challenging due to their complex synthesis. Additionally, the reversible hydrogenation and

dehydrogenation processes remain relatively underexplored, and improving the efficiency of these reactions at lower temperatures is an urgent challenge. The development of more efficient catalysts and optimized reaction conditions, while simultaneously reducing the overall cost of dehydrogenation, are critical goals for the future.

Based on the current findings, several directions for future research are evident. First, in terms of catalyst design, there is a need for the development of novel bimetallic and single-atom catalysts, particularly in the realm of reversible addition and dehydrogenation. These new catalysts should not only improve catalytic activity and stability but also help drive down costs. Second, a deeper understanding of the reaction mechanisms involved in LOHCs is crucial to optimizing reaction conditions for efficient hydrogen storage, particularly at lower temperatures. Finally, the development of environmentally friendly and sustainable catalysts, along with thorough risk assessments and economic evaluations of LOHCs, will be key to making this technology more practical and commercially viable. Collaborative efforts between the scientific community and industry will be essential to ensure that LOHCs become a widely adopted technology in the future.

Data availability

Data sharing is not applicable to this review as no primary research results, software or code have been included and no new data were generated or analyzed.

Author contributions

Meiying Dai: formal analysis, investigation, methodology, writing – original draft, writing – review & editing. Yibo Qin: formal analysis, methodology. Longfei Chen: methodology; Xinqing Chen: supervision, methodology, funding acquisition, writing – review & editing.

Conflicts of interest

There are no conflicts to declare.

Acknowledgements

This work was supported by the National Key Research and Development Program of China (2022YFE0208300) and the Natural Science Foundation of China (22078354).

References

1 J. Graetz, *Chem. Soc. Rev.*, 2009, **38**, 73–82.
2 T. He, P. Pachfule, H. Wu, Q. Xu and P. Chen, *Nat. Rev. Mater.*, 2016, **1**, 16059.
3 Y.-Q. Zou, N. Von Wolff, A. Anaby, Y. Xie and D. Milstein, *Nat. Catal.*, 2019, **2**, 415–422.
4 Y. Guo, M. Wang, Q. Zhu, D. Xiao and D. Ma, *Nat. Catal.*, 2022, **5**, 968–968.
5 L. Ge, M. Qiu, Y. Zhu, S. Yang, W. Li, W. Li, Z. Jiang and X. Chen, *Appl. Catal., A*, 2022, **319**, 121958.
6 O. Sultan and H. Shaw, *NASA STI/recon technical report N*, 1975, vol. 76, pp. 33642–33645.
7 D. Teichmann, W. Arlt, P. Wasserscheid and R. Freymann, *Energy Environ. Sci.*, 2011, **4**, 2767.
8 S. Lee, T. Kim, G. Han, S. Kang, Y.-S. Yoo, S.-Y. Jeon and J. Bae, *Renewable Sustainable Energy Rev.*, 2021, **150**, 111447.
9 P. Rao and M. Yoon, *Energies*, 2020, **13**, 6040.
10 R. B. Biniwale, N. Kariya, H. Yamashiro and M. Ichikawa, *J. Phys. Chem. B*, 2006, **110**, 3189–3196.
11 Z. Chen, M. Yang, T. Zhu, Z. Zhang, X. Chen, Z. Liu, Y. Dong, G. Cheng and H. Cheng, *Int. J. Hydrogen Energy*, 2018, **43**, 12688–12696.
12 L. Zhang, X. Wang, Y. Xue, X. Zeng, H. Chen, R. Li and S. Wang, *Catal. Sci. Technol.*, 2014, **4**, 1939–1948.
13 M. Yang, X. Xing, T. Zhu, X. Chen, Y. Dong and H. Cheng, *J. Energy Chem.*, 2020, **41**, 115–119.
14 L. Shi, X. Liu, Y. Tuo, J. Xu, P. Li and Y. Han, *Int. J. Hydrogen Energy*, 2017, **42**, 17403–17413.
15 M. Kosaka, T. Higo, S. Ogo, J. G. Seo, S. Kado, K. Imagawa and Y. Sekine, *Int. J. Hydrogen Energy*, 2020, **45**, 738–743.
16 R. Biniwale, S. Rayalu, S. Devotta and M. Ichikawa, *Int. J. Hydrogen Energy*, 2008, **33**, 360–365.
17 M. Yang, Y. Dong and H. S. Cheng, *Adv. Mater. Res.*, 2014, **953–954**, 981–984.
18 K. M. Eblagon, D. Rentsch, O. Friedrichs, A. Remhof, A. Zuettel, A. J. Ramirez-Cuesta and S. C. Tsang, *Int. J. Hydrogen Energy*, 2010, **35**, 11609–11621.
19 Q. Pei, J. Yu, G. Qiu, K. C. Tan, J. Wen, Y. Yu, J. Wang, J. Guo, J. Guo, L. Rao, T. He and P. Chen, *Appl. Catal., B*, 2023, **336**, 122947.
20 Y. Wu, H. Yu, Y. Guo, Y. Zhang, X. Jiang, B. Sun, K. Fu, J. Chen, Y. Qi, J. Zheng and X. Li, *J. Mater. Chem. A*, 2019, **7**, 16677–16684.
21 H. Yu, Y. Wu, S. Chen, Z. Xie, Y. Wu, N. Cheng, X. Yang, W. Lin, L. Xie, X. Li and J. Zheng, *Appl. Catal., B*, 2022, **317**, 121720.
22 K. M. Eblagon, K. Tam, K. M. K. Yu and S. C. E. Tsang, *J. Phys. Chem. C*, 2012, **116**, 7421–7429.
23 D. Forberg, T. Schwob, M. Zaheer, M. Friedrich, N. Miyajima and R. Kempe, *Nat. Commun.*, 2016, **7**, 13201.
24 H. Liu, C. Zhou, W. Li, W. Li, M. Qiu, X. Chen, H. Wang and Y. Sun, *ACS Sustainable Chem. Eng.*, 2021, **9**, 5260–5267.
25 X. Ye, Y. An and G. Xu, *J. Alloys Compd.*, 2011, **509**, 152–156.
26 B. Wang, S. Wang, S. Lu, P. Li and T. Fang, *Fuel*, 2023, **339**, 127338.
27 B. Wang, Q. Dong, S.-Y. Wang, P.-Y. Li, S.-Y. Wang, S.-H. Lu and T. Fang, *Front. Chem.*, 2022, **10**, 1081319.
28 B. Chen, B. Hui, Y. Dong, Q. Sheng, X. Li, Q. Hao and C. Liu, *Fuel*, 2022, **324**, 124405.
29 H. Yu, X. Yang, Y. Wu, Y. Guo, S. Li, W. Lin, X. Li and J. Zheng, *J. Energy Chem.*, 2020, **40**, 188–195.
30 Y. Wu, Y. Guo, H. Yu, X. Jiang, Y. Zhang, Y. Qi, K. Fu, L. Xie, G. Li, J. Zheng and X. Li, *CCS Chem.*, 2021, **3**, 974–984.
31 Y. Qin and X. Bai, *Catal. Sci. Technol.*, 2022, **12**, 2829–2836.

32 Y. Tian, H. Duan, B. Zhang, S. Gong, Z. Lu, L. Dai, C. Qiao, G. Liu and Y. Zhao, *Angew. Chem., Int. Ed.*, 2021, **60**, 21713–21717.
33 B. Pawelec, R. Mariscal, R. M. Navarro, S. Van Bokhorst, S. Rojas and J. L. G. Fierro, *Appl. Catal., A*, 2002, **225**, 223–237.
34 K. M. Eblagon, K. Tam and S. C. E. Tsang, *Energy Environ. Sci.*, 2012, **5**, 8621.
35 A.-G. A. Ali, L. I. Ali, S. M. Aboul-Fotouh and A. K. Aboul-Gheit, *Appl. Catal., A*, 1998, **170**, 285–296.
36 M. Mateen, K. Shah, Z. Chen, C. Chen and Y. Li, *Nano Res.*, 2019, **12**, 1631–1634.
37 S. Lu, W. Lonergan, J. Bosco, S. Wang, Y. Zhu, Y. Xie and J. Chen, *J. Catal.*, 2008, **259**, 260–268.
38 T. Liu, W. Wu and X. Bai, *Ultrason. Sonochem.*, 2024, **105**, 106861.
39 T. Zhu, L. Liu, Y. Zhao, M. Gao, Y. Dong, D. Xia, P. Huang, H. Cheng and M. Yang, *Chem. Eng. J.*, 2024, **493**, 152354.
40 D. Forberg, T. Schwob, M. Zaheer, M. Friedrich, N. Miyajima and R. Kempe, *Nat. Commun.*, 2016, **7**, 13201.
41 L. Ge, Y. Zhu, M. Qiu, S. Yang, N. Sun, W. Wei, J. Li and X. Chen, *Appl. Catal., B*, 2023, **333**, 122793.
42 B. Wang, Y.-T. Chen, T.-Y. Chang, Z. Jiang, Z.-Q. Huang, S.-Y. Wang, C.-R. Chang, Y.-S. Chen, J.-J. Wei, S. Yang and T. Fang, *Appl. Catal., B*, 2020, **266**, 118658.
43 Y. Li, J. Ye, T. Xu, G. Xia and X. Yu, *Int. J. Hydrogen Energy*, 2024, **65**, 769–778.
44 R. Biniwale, S. Rayalu, S. Devotta and M. Ichikawa, *Int. J. Hydrogen Energy*, 2008, **33**, 360–365.
45 Z. Jiang, X. Gong, B. Wang, Z. Wu and T. Fang, *Int. J. Hydrogen Energy*, 2019, **44**, 2951–2959.
46 M. Yang, Y. Dong, S. Fei, H. Ke and H. Cheng, *Int. J. Hydrogen Energy*, 2014, **39**, 18976–18983.
47 B. Wang, T. Yan, T. Chang, J. Wei, Q. Zhou, S. Yang and T. Fang, *Carbon*, 2017, **122**, 9–18.
48 B. Wang, T. Chang, Z. Jiang, J. Wei, Y. Zhang, S. Yang and T. Fang, *Int. J. Hydrogen Energy*, 2018, **43**, 7317–7325.
49 B. Wang, T. Chang, Z. Jiang, J. Wei and T. Fang, *Appl. Catal., B*, 2019, **251**, 261–272.
50 B. Wang, T. Chang, X. Gong, Z. Jiang, S. Yang, Y. Chen and T. Fang, *ACS Sustainable Chem. Eng.*, 2019, **7**, 1760–1768.
51 Z. Wei, X. Bai, A. L. Maximov and W. Wu, *Ultrason. Sonochem.*, 2024, **103**, 106793.
52 C. Sun, X. Liu and X. Bai, *Int. J. Hydrogen Energy*, 2024, **49**, 1547–1557.
53 Z. Jiang, X. Gong, S. Guo, Y. Bai and T. Fang, *Int. J. Hydrogen Energy*, 2021, **46**, 2376–2389.
54 C. Li, G. Yang, F. Li, T. Zhu, M. Zhang, J. Zhang, Y. Dong and M. Yang, *Appl. Catal., B*, 2025, **365**, 124980.
55 T. Zhu, R. Wang, Z. Chen, F. Ji, Y. Dong and M. Yang, *Catal. Sci. Technol.*, 2022, **12**, 4763–4775.
56 V. Sage, J. Patel, P. Hazewinkel, Q. U. A. Yasin, F. Wang, Y. Yang, K. Kozielski and C. Li, *Int. J. Hydrogen Energy*, 2024, **56**, 1419–1434.
57 Y. Li, X. Guo, S. Zhang and Y. He, *Energy Fuels*, 2024, **38**, 12447–12471.
58 C.-I. Ahn, Y. Kwak, A.-R. Kim, M. Jang, A. Badakhsh, J. Cha, Y. Kim, Y. S. Jo, H. Jeong, S. H. Choi, S. W. Nam, C. W. Yoon and H. Sohn, *Appl. Catal., B*, 2022, **307**, 121169.
59 S. Han, C. Ahn, B. J. Shim, E. On, C. Kim, H. Sohn, H. Jeong, Y. Kim and C. W. Yoon, *Chem. Eng. J.*, 2024, **487**, 150446.
60 Z. Tan, G. Fan, L. Zheng and F. Li, *ACS Catal.*, 2024, **14**, 11218–11230.
61 L. Li, Z. Yang, X. Yang, H. Xiong, Z. Jiang and T. Fang, *Chem. Eng. J.*, 2024, **492**, 152089.
62 Z. Zhang, T. Liu, X. Zhang, C. Zhang, X. Jin, J. Zheng and Q. Sun, *ACS Appl. Mater. Interfaces*, 2024, **16**, 37963–37971.
63 J. Gao, N. Li, D. Zhang and Y. Zhao, *Int. J. Hydrogen Energy*, 2024, **85**, 865–880.
64 J. Gao, N. Li, D. Zhang, H. Ma, X. Zhan, S. Zhao and Y. Zhao, *Mol. Catal.*, 2024, **560**, 114148.
65 C. Li, Q. Zhang, Z. Xu, L. Liu, T. Zhu, Z. Chen, Y. Dong and M. Yang, *Int. J. Hydrogen Energy*, 2023, **48**, 90–100.
66 J. Lee, B. G. Park, K. Sung, H. Lee, J. Kim, E. Nam, J. W. Han and K. An, *ACS Catal.*, 2023, **13**, 13691–13703.
67 T. Zhu, M. Yang, X. Chen, Y. Dong, Z. Zhang and H. Cheng, *J. Catal.*, 2019, **378**, 382–391.
68 X. Yang, Y. Wu, H. Yu, M. Sun, J. Zheng, X. Li, W. Lin and Y. Wu, *Int. J. Hydrogen Energy*, 2020, **45**, 33657–33662.
69 X. Zhang, N. He, L. Lin, Q. Zhu, G. Wang and H. Guo, *Catal. Sci. Technol.*, 2020, **10**, 1171–1181.
70 Y. Okada, E. Sasaki, E. Watanabe, S. Hyodo and H. Nishijima, *Int. J. Hydrogen Energy*, 2006, **31**, 1348–1356.
71 L. Shi, S. Qi, J. Qu, T. Che, C. Yi and B. Yang, *Int. J. Hydrogen Energy*, 2019, **44**, 5345–5354.
72 L. Chen, P. Verma, K. Hou, Z. Qi, S. Zhang, Y.-S. Liu, J. Guo, V. Stavila, M. D. Allendorf, L. Zheng, M. Salmeron, D. Prendergast, G. A. Somorjai and J. Su, *Nat. Commun.*, 2022, **13**, 1092.
73 P. Hu, E. Fogler, Y. Diskin-Posner, M. A. Iron and D. Milstein, *Nat. Commun.*, 2015, **6**, 6859.
74 D. Forberg, T. Schwob, M. Zaheer, M. Friedrich, N. Miyajima and R. Kempe, *Nat. Commun.*, 2016, **7**, 13201.
75 W. Xue, H. Liu, B. Mao, H. Liu, M. Qiu, C. Yang, X. Chen and Y. Sun, *Chem. Eng. J.*, 2021, **421**, 127781.
76 H. Yu, X. Yang, X. Jiang, Y. Wu, S. Chen, W. Lin, Y. Wu, L. Xie, X. Li and J. Zheng, *Nano Energy*, 2021, **80**, 105476.
77 H. Yu, Z. Zhang, X. Jin, X. Zhang, R. Jin, Y. Lin, Z. Xie, Y. Huang, T. Liu, X. Li, Q. Sun and J. Zheng, *ACS Catal.*, 2024, **14**, 10519–10528.
78 W. Xue, B. Zhao, H. Liu, X. Chen and L. Liu, *Appl. Catal., B*, 2024, **343**, 123574.
79 W. Xue, H. Liu, B. Zhao, L. Ge, S. Yang, M. Qiu, J. Li, W. Han and X. Chen, *Appl. Catal., B*, 2023, **327**, 122453.
80 Y. Wu, Y. Guo, H. Yu, X. Jiang, Y. Zhang, Y. Qi, K. Fu, L. Xie, G. Li, J. Zheng and X. Li, *CCS Chem.*, 2021, **3**, 974–984.